

1 **Characteristics of Trace Metals in Traffic-Derived Particles in**

2 **Hsuehshan Tunnel, Taiwan: Size Distribution, Potential Source, and**

3 **Fingerprinting Metal Ratio**

4 **Yu-Chi Lin^{1*}, Chuen-Jinn Tsai², Yueh-Chuen Wu³, Renjiang Zhang⁴, Kai-Hsien**

5 **Chi⁵, Yi-Tang Huang¹, Shuen-Hsin Lin¹, Shih-Chieh Hsu¹**

6
7 *¹Research Center for Environmental Changes, Academia Sinica, Nankang, Taipei, 115,*
8 *Taiwan.*

9 *²Institute of Environmental Engineering, National Chiao Tung University,*
10 *Hsinchu, 300, Taiwan.*

11 *³Environmental Analysis Laboratory, Environmental Protection Administration,*
12 *Executive Yuan, 320, Taiwan.*

13 *⁴Key Laboratory of Regional Climate-Environment Research for Temperate East Asia,*
14 *Institute of Atmospheric Physics, Chinese Academy of Sciences, Beijing, China.*

15 *⁵Institute of Environmental and Occupational Health Sciences, National Yang Ming*
16 *University, Taipei 112, Taiwan*

17
18 *Corresponding author: Yu-Chi Lin

19 Phone: +886-2-26539885 ext. 436

20 Fax: +886-2-27833584

21 E-mail: schsu815@rcec.sinica.edu.tw; yclin26@rcec.sinica.edu.tw

22

1 **Abstract**

2 Traffic emissions are a significant source of airborne particulate matter (PM) in
3 ambient environments. These emissions contain high abundance of toxic metals and
4 thus pose adverse effects on human health. Size-fractionated aerosol samples were
5 collected from May to September 2013 by using micro-orifice uniform deposited
6 **impactors** (MOUDI). Sample collection was conducted simultaneously at the inlet
7 and outlet sites of Hsuehshan Tunnel in northern Taiwan, which is the second
8 longest freeway tunnel (12.9 km) in Asia. Such endeavor aims to characterize the
9 chemical constituents and size distributions, as well as fingerprinting ratios of
10 particulate metals emitted by vehicle fleets. A total of 36 metals in size-resolved
11 aerosols were determined through inductively coupled plasma mass spectrometry.
12 Three major groups, namely, tailpipe emissions (Zn, Pb, and V), wear debris (Cu, Cd,
13 Fe, Ga, Mn, Mo, Sb, and Sn), and resuspended dust (Ca, Mg, K, and Rb), of
14 airborne PM metals were categorized on the basis of the results of enrichment factor,
15 correlation matrix, and principal component analysis. Size distributions of
16 wear-originated metals resembled the pattern of crustal elements, which were
17 predominated by super-micron particulates (PM₁₋₁₀). By contrast, tailpipe exhaust
18 elements such as Zn, Pb, and V were distributed mainly in submicron particles. By
19 employing Cu as a tracer of wear abrasion, several inter-metal ratios, including
20 Fe/Cu (14), Ba/Cu (1.05), Sb/Cu (0.16), Sn/Cu (0.10), and Ga/Cu (0.03), served as
21 fingerprints for wear debris. **However, the data set collected in this work is useful**
22 **for further studies on traffic emission inventory and human health effects of**
23 **traffic-related PM**

24

25 **Keywords:** Traffic-related Metal, Size-fractionated Aerosol, Fingerprinting Metal

1. Introduction

Traffic emissions are an important source of **particulate matter** (PM) (Sternbeck et al., 2002; Birmili et al., 2006; Lough et al., 2005; Johansson et al., 2009) in urban atmosphere. Exposure to traffic-derived PM poses adverse effects on human health and increases the risk of respiratory illness, cardiovascular diseases, and asthma (Brauer et al., 2002; Defino et al., 2005), resulting in increased mortality (Nel, 2005). Airborne traffic-related PM is emitted mainly by tailpipe exhaust from gasoline and diesel engines (exhaust emissions), wear from brake linings and tires, as well as re-suspension of road dust (non-exhaust emissions) by moving vehicles (Rogge et al., 1993; Cadle et al., 1999; Garg et al., 2000; Wåhlin et al., 2006; Lawrence et al., 2013). Exhaust emissions contribute a large amount of fine **particulate matter** (aerodynamic diameter less than 2.5 μm , $\text{PM}_{2.5}$), whereas non-exhaust emissions mainly consist of **larger particles** (Abu-Allaban et al., 2002; Sanders et al., 2003). With regard to elemental compositions, Pb, Zn, Ni, and V in submicron particles were commonly attributed to pipe emissions and fuel oil combustion of both gasoline and diesel engines **as shown in Table S1** (Lin et al., 2005; Wang et al., 2003; Shafer et al., 2012). Silicon (Si), Fe, Ca, Na, Mg, Al, and K are essentially found in **larger particles** and are associated with re-suspension of road dust. Large amounts of Ca and K observed in submicron particles occasionally originate from the tailpipe emission of lubricating oil as well as the vaporization of volatile K-compounds and potassium titanate ($\text{K}_2\text{O}\cdot\text{nTiO}_2$), which is used for improving heat resistance and wear characteristics (Hee and Filip, 2005; Iijima et al., 2007; Kuo et al., 2009). Meanwhile, Cu, Ba, Sb, Fe, Cd, Cr, Ga, Sn, and Zn, which are commonly associated with wear dust from brake

1 linings and tires, are predominant in coarse PM (Lough et al., 2005; Grieshop et al.,
2 2006; Thorpe and Harrison, 2008).

3 A number of studies investigated the chemical and physical properties of
4 traffic-originated PM by performing conventional dynamometric tests and field
5 measurements near roads and inside tunnels (Sternbeck et al., 2002; Sanders et al.,
6 2003; Birmili et al., 2006; Wählín et al., 2006; Iijima et al., 2007; Ning et al., 2007;
7 Harrison et al., 2012; Dall'Osto et al., 2013; Lawrence et al., 2013). Dynamometric
8 tests may allow optimal control of experimental conditions; however, the limitations
9 of such tests are the costs and inadequate representative of real-world traffic
10 emissions on the roads (Jamriska et al., 2004). A field measurement nearby roadside
11 is another method to well characterize the traffic-derived PM (Ning et al., 2004), but it
12 may be influenced by local meteorological conditions and traffic activities (Jamriska
13 et al., 2004; Ntziachristos et al., 2007). Accordingly, tunnel study may be an
14 alternative way to address this issue.

15 Tunnel aerosol sampling is designed to explore size distributions, chemical
16 compositions, and emission factors of traffic-related aerosols and their associated
17 compositions (Weingartner et al., 1997; Funasaka et al., 1998; Gillies et al., 2001;
18 Sternbeck et al., 2002; Grieshop et al., 2006; Chiang and Huang, 2009; Pio et al.,
19 2013). Pio et al. (2013) discriminated three main types of aerosols in Marquês tunnel,
20 Portugal, namely, carbonaceous, soil component, and vehicle mechanical wear. They
21 also suggested that Cu is a good tracer for wear emissions of road traffic. Wear
22 emission elements such as Zn, Sb, and Ba exhibited a peak mode in the size range of
23 3.2 μm to 5.6 μm . In comparison, Pb, Ca, and Fe partitioned within 0.1 μm are mostly
24 emitted from combustion of fuel and lubricant oil or vaporization from hot brake
25 surface (Lough et al., 2005). Sternbeck et al. (2002) collected aerosol samples in two

1 tunnels in Sweden and analyzed trace metals through inductively coupled plasma
2 mass spectrometry (ICP-MS). They concluded that vehicle-related metals, such as Cu,
3 Zn, Cd, Sb, Ba, and Pb, originated mainly from wear rather than from combustion,
4 and that heavy-duty vehicles (HDV), rather than light-duty vehicles (LDV), are the
5 leading emitter of Ba and Sb. They further suggested that a Sb/Cu ratio of ~0.22
6 indicates the presence of brake wear-related particles.

7 In this work, a series of aerosol sampling was conducted at two sites in
8 Hsuehshan Tunnel by using micro-orifice uniform deposited impactors (MOUDI) to
9 characterize the physical and chemical properties of metallic aerosols under real
10 driving conditions. In the past several intensive measurements of aerosols have been
11 carried out inside Hsuehshan Tunnel (Chang et al., 2009; Chen et al., 2010; Cheng et
12 al., 2010a; Zhu et al., 2010); for instance, Zhu et al. (2010) characterized different
13 temperature carbonaceous aerosols in fine PM and then identified their sources by
14 positive matrix factorization (PMF) approach. Moreover, number concentrations of
15 ultrafine particle (UFP) measured by Cheng et al. (2010) indicate that UFP, on
16 average, were about $1.0 \times 10^5 - 3.0 \times 10^5$ particles/cm³ while higher UFP numbers
17 were found at a traffic jam. They also suggested that gas-to-particle conversion is a
18 crucial way to produce nucleation PM at entrance of the tunnel, and coagulation
19 growth of nucleation particles is an important mechanism for forming Aitken mode
20 PM at the middle and exit section. Besides, gaseous pollutants, including VOC, O₃,
21 CO and NO_x, inside this tunnel have been also studied previously (Chang et al., 2009;
22 Li et al., 2011, Lai and Peng, 2012). Thus, Hsuehshan Tunnel is a suitable study area
23 for characterizing the behaviors of air pollutants associated with vehicle fleets. During
24 the experimental campaigns, a total of 24 sets of size-resolved aerosol samples were
25 collected; 36 target metals were analyzed by ICP-MS. Elemental compositions, size

1 distributions, and fingerprinting metal ratios in traffic aerosols are reported in this
2 paper. The resulting comprehensive dataset would provide useful insight into health
3 effect studies, source apportionment of atmospheric metals, and emissions inventory
4 of traffic-related particulate metals.

5

6 **2. Methodology**

7 **2.1 Site description**

8 With a length of 12.9 km, Hsuehshan Tunnel is the second longest road tunnel
9 in Asia and the fifth longest in the world. Opened to traffic on June 2006, Hsuehshan
10 Tunnel connects Pingling in New Taipei City and Toucheng in Yilan County. The
11 tunnel has two separate two-lane bores and ascends steadily from 44 m a.m.s.l.
12 (meters above mean sea level) at the south end (Toucheng) to 208 m a.m.s.l. at the
13 north end (Pingling), that is, a slope of 1.26 %. Only passenger cars and light-duty
14 trucks (which are both classified under LDV) as well as shuttle buses (categorized
15 under HDV) are allowed to travel inside the tunnel with vehicle speed limited to 90
16 km/h. Four aerosol sampling campaigns were conducted in the northbound bore
17 between May and September 2013; each campaign lasted for three days: Friday to
18 Sunday. During the sampling period, the traffic volume passing through Hsuehshan
19 Tunnel at the northbound, in general, approximated 1800 vehicles per hour on the
20 weekend, which was 1.3 times higher than the workdays (see in Table 1). However,
21 the traffic flow increased to 2300 vehicles/h from Sunday afternoon to evening when
22 people traveled back to Taipei, as a result, a traffic jam always occurred inside the
23 tunnel since Sunday afternoon, probably influencing traffic-related PM metal
24 emissions.

25 A ventilation system composed of three air exchange stations and three air

1 interchange stations was built inside the tunnel to maintain air quality. Exchange and
2 interchange stations are located alternatively at intervals of nearly 2 km. In exchange
3 stations, polluted air is exchanged with outer fresh air by using separate fresh and
4 exhaust shafts equipped with two sets of fans. Fans are typically triggered at
5 temperatures higher than 40 °C or CO concentrations higher than 75 ppm. In
6 interchange stations, the air in each bore is diverted into another bore by two sets of
7 fans, which are also triggered when CO concentration exceeds 75 ppm. **During the**
8 **sampling periods, the ventilation system operated regularly, particular in July and**
9 **August campaigns with the temperature near the outlet site frequently more than 40**
10 **°C.**

11

12 **2.2 Sampling and analysis**

13 During the sampling campaigns, two aerosol samplers were installed at 1.7 and
14 10.6 km from the entrance. **The intakes of both aerosol instruments were placed 1.6 m**
15 **above the pavement.** MOUDIs (model 100, MSP Corporation, Minneapolis,
16 Minnesota) equipped with pre-weighed Teflon filters (PTFE, 47 mm in diameter and
17 1.0 mm in pore size, Pall Gelman, East Hills, New York) were used to collect
18 size-resolved aerosol samples. MOUDI consists of 10 size-fractionating stages with
19 50 % cut-off diameters of 10, 5.6, 3.2, 1.8, 1.0, 0.56, 0.32, 0.18, 0.10, and 0.056 μm ,
20 plus an inlet (nominal cut size of 18 μm) and an after-filter ($< 0.018 \mu\text{m}$) at the base.
21 Flow rate was calibrated prior to each sampling run and maintained at 30 L/min. Each
22 sample was collected for 12 h (typically from 9 a.m. to 9 p.m.) daily.

23 After sampling, filter samples were conditioned for 48 h, followed by gravimetric
24 measurement at 23 °C and RH $30 \pm 5\%$ with a microbalance (METTLER TOLEDO,
25 MX5, AX205, precision 1 μg) to determine the net mass of collected aerosol particles,

1 which is needed to calculate the PM mass concentration. The samples were then
2 subjected to acid digestion with the use of an ultra-high throughput microwave
3 digestion system (MARSPress, CEM Corporation, Matthews, NC). The vessels
4 were acid-cleaned thoroughly prior to sample digestion. A half of each sample filter
5 was digested in an acid mixture (1.5 ml 60% HNO₃ and 1.5 ml 48% HF). After
6 digestion, the vessels were transferred to the XpressVapTM accessory sets (CEM) for
7 evaporation of the remaining acids. When nearly dried, 2 mL concentrated HNO₃ was
8 added into each vessel and reheated. The resulting solution was then diluted with
9 Milli-Q water to a final volume of 15 mL for analysis. The digestion procedure has
10 been detailed in previous studies (Hsu et al., 2008; 2009; Zhang et al., 2013).

11 A total of 36 target elements in aerosols were analyzed by ICP-MS (Elan 6100,
12 Perkin ElmerTM SCIEX, USA). For each run, a blank reagent and three filter
13 membrane blanks were subjected to the same procedure as that for the samples.
14 Indium (In) was added to the digests as an internal standard with a final concentration
15 of 10 ng/mL for ICP-MS analysis. The QA/QC of data is guaranteed by the analysis
16 of a standard reference material, SRM 1648 (urban atmospheric particulate matter
17 prepared by the National Institute Standards and Technology (NIST)). The recoveries
18 of target elements mostly fell within 10 % (n = 7) of certified or reference values
19 (Table S2). **The method detection limits (MDLs) for the analyzed elements are also**
20 **presented.** Details of the ICP-MS analysis has been extensively discussed by Hsu et al.
21 (2010) and Zhang et al (2013).

22

23 **2.3 Enrichment factor and principal component analysis**

24 In addition to size distribution, three approaches, namely, enrichment factor (EF),
25 correlation matrix, and principal component analysis (PCA) were applied to explore

1 the possible sources and associations of elements. EF is used to assess the influence of
2 crustal source on a given metal (X_i), which can be calculated by using the following
3 equation:

$$4 \quad EF(X_i) = \frac{(X_i / Al)_{PM}}{(X_i / Al)_{Crust}} \quad (1)$$

6 where $(X_i/Al)_{PM}$ is the concentration ratio of a given element X to Al in tunnel
7 particulate matters and $(X_i/Al)_{crust}$ is the concentration ratio of an interested element X
8 to Al in the average crustal abundance (Taylor, 1964).

9 PCA can elucidate variance in a given dataset in terms of minimum number of
10 significant component. This technique has been employed in the tunnel studies
11 concerning source apportionment of airborne metals (Lin et al., 2005; Lawrence et al.,
12 2013). The software used here is STATISTICA 12 (Statsoft Inc.). A factor loading of >
13 0.7 was adopted in this study to assign source identification to a given principal
14 component.

15

16 **3. Result and Discussions**

17 **3.1 Chemical compositions**

18 Table 1 summarizes the data on PM mass concentrations in size-resolved
19 aerosols at both the inlet and outlet sites in Hsuehshan Tunnel. The aerosols are
20 treated into three size bins: submicron (PM_1), fine ($PM_{1-1.8}$), and coarse ($PM_{1.8-10}$)
21 modes. During the sampling periods, the mass concentrations of PM_{10} , which were
22 determined as the sum of aerosol masses at all corresponding stages with a cut-off
23 diameter less than 10 μm , ranged from 35 to 68 $\mu g/m^3$ (average: $54 \pm 9 \mu g/m^3$) at the
24 inlet site and from 106 to 241 $\mu g/m^3$ (average: $162 \pm 42 \mu g/m^3$) at the outlet site.
25 Submicron particles were the predominant fraction, accounting for $60 \pm 6 \%$ and 82

1 ± 3 % of PM_{10} mass at the entrance and the exit, respectively. The abundance of
2 submicron PM may indicate that combustion processes are significant sources of
3 tunnel aerosols, which are presumably dominated by carbonaceous particles (Zhu et
4 al., 2010; Pio et al., 2013). Compared with the inlet site, higher concentrations of
5 $PM_{1-1.8}$ and PM_1 were observed at the outlet site by a factor of 2.5 and 4.4,
6 respectively. For $PM_{1.8-10}$, the concentration at the outlet site was nearly equal to that
7 at the inlet site (outlet-to-inlet ratio: ~ 1.1). The outlet-to-inlet ratio of PM mass
8 concentration increases with decreasing PM size, indicating that smaller particles are
9 relatively efficiently transported from the entrance to the exit; previous studies have
10 attributed such efficient transport to “piston effect” (Chang et al., 2009; Cheng et al.,
11 2010; Moreno et al., 2014). These authors suggested that passing vehicles pick up
12 air pollutants emitted from vehicle fleets and the flows lead them to the exit,
13 resulting in the accumulation of large quantities of air pollutants in that area.

14 Figure 1a shows the average elemental concentrations of PM_{10} at the two sites
15 in Hsuehshan Tunnel, and Figure 1b depicts the partitioning of trace elements
16 among three size bins. As shown in Figure 1a, Fe was the most abundant element,
17 with a mean concentration of 2384 ± 1416 ng/m³. In addition to Na, Ca, and Al (300
18 to 500 ng/m³), Zn, K, Ba, Cu, and Mg (up to 100 ng/m³) were also major metals in
19 PM_{10} , followed by Ti (73 ng/m³), Mn (29 ng/m³), Sb (23 ng/m³), and then followed
20 by Mo, Pb, Ga, Sr, Ni, V, and Ce (1 ng/m³ to 10 ng/m³). The rest of the elements
21 have concentrations less than 1 ng/m³ (i.e., 0.9 ng/m³ for Bi to 0.02 ng/m³ for U).
22 Most elements exhibited significantly higher concentrations at the exit than at the
23 entrance ($p < 0.05$, Figure 1c), with the exception of a number of crustal elements
24 such as Al, K, Mg, and Rb. This suggests that a lower road dust reservoir is present
25 inside the freeway tunnel (Amato et al., 2012). Considerably high outlet-to-inlet

1 ratios (ranging from 2.2 for Sr to 4.3 for Zn) were found for traffic-derived elements,
2 including Zn, Cu, Ba, Mn, Sb, Sn, Pb, Ga, Sr, and Cd.

3

4 **3.2 Size distributions**

5 The average size distributions of some of the analyzed metals are shown in
6 Figures 1b, 2 and S1. Barium (Ba), Cd, Cu, Fe, Ga, Mn, Mo, Sb, and Sn were
7 predominant in coarse mode **at the inlet site** (Figure 1b). These elements displayed a
8 typical mono-modal distribution with a major peak in the size range of 3.2 - 5.6 μm ,
9 while they had another small peak at 1.0 - 1.8 μm at times (Figures 2 and S2). The
10 size distribution patterns of these metals were consistent with the results observed by
11 Harrison et al. (2012) at a curbside in central London. The authors assigned the
12 elements Fe, Cu, Sb, Ba, and Zn to the non-exhaust traffic particles. At the outlet site,
13 those elements (Ba, Cd, Cu, Fe, Ga, Mn, Mo, Sb, and Sn) similarly had a
14 mono-modal size distribution, but the main peak shifted to 1.0 - 1.8 μm (Figures 2
15 and S2). Similar to that in PM, this shift was perhaps due to “piston effect,” which,
16 as previously mentioned, facilitated the transport of finer PM to the exit.

17 Zinc (Zn) showed a bi-modal distribution for most samples at the entrance, with
18 a major peak in the size range of 3.2 - 5.6 μm and a second peak in the size range of
19 0.56 - 1.0 μm . Meanwhile, a mono-modal pattern with a major peak at 1.0 - 1.8 μm
20 was found at the exit. Lead (Pb) displayed two peaks at the inlet site: one at 0.56 -
21 1.0 μm and another one at 3.2 - 5.6 μm . However, Pb exhibited a typical
22 mono-modal distribution at the outlet site, peaking at 0.32 - 0.56 μm . Vanadium (V)
23 revealed a bi-modal size pattern with a major peak at 0.32 - 0.56 μm and a second
24 peak at 3.2 - 5.6 μm at the inlet site, whereas it peaked at 0.18 - 0.32 μm or 0.32 -
25 0.56 μm at the exit.

1 Aluminum (Al), Ca and Mg of predominant geological origins showed a
2 typical mono-modal size distribution at the inlet site with a major peak at 3.2 - 5.6
3 μm ; however, a peak was occasionally found in the submicron particles (Figures S1
4 and S3). For example, the abundance of Al, Ca and K was observed at submicron
5 size in two sets of samples (July 21 and August 10). Such abundance was ascribed to
6 non-crustal sources such as vaporization from lubricating oil and diesel emissions
7 (Wang et al., 2003), which perhaps alters the size distributions of these crustal
8 elements. Submicron mode, which is an indicator of combustion or high temperature
9 processes, contributes non-negligible Ca and K, which are usually regarded as
10 crustal elements. Potassium titanate and a number of volatile compounds are known
11 to contain K and are therefore may be the possible sources of submicron K (Hee and
12 Filip, 2005; Iijima et al., 2007). Submicron Ca probably originated from tailpipe
13 emissions of lubricating oil (Kuo et al., 2009). Like traffic elements, these crustal
14 elements had a major peak that shifted to 1.0 - 1.8 μm at the outlet site, which was
15 also arisen from the "piston effect". At the inlet site, rare earth elements (REEs),
16 such as La, Ce, Nd, Pr, and Sm, revealed a mono-modal size distribution with a
17 major peak at 3.2 - 5.6 μm . At the exit, such elements essentially showed a
18 mono-modal distribution that peaked at 1.0 - 1.8 μm .

19

20 **3.3 Sources of trace metals**

21 Figure 3 presents the results of enrichment factor analysis for all analyzed
22 elements in three size bins of size-segregated particles at both the inlet and outlet sites.
23 EF values for all species were higher at the outlet than at the inlet site, suggesting that
24 the influence of re-suspended road dust were insignificant for most metals at the exit.
25 Enrichment factor values for Ca, K, Mg, Rb, Sr, and Ti in the three size-resolved

1 particles were generally close to unity at both sites, demonstrating that these elements
2 originated mainly from the resuspension of soil and road dust. EF values for these
3 geological metals increased with decreasing size, indicating that these elements in
4 smaller particles would be significantly influenced by anthropogenic sources such as
5 diesel emissions, lubricating oil, and additive in oil fuels. For lanthanides, lower
6 enrichment was found for La, Pr, Nd, and Sm in all three sized PM, although high EFs
7 were occasionally found. This indicates that although such elements mainly originate
8 from geological sources, they sometimes from mixed sources of dust and
9 anthropogenic emissions such as automotive catalyst (Kulkarni et al., 2006). Cerium
10 (Ce), which is one of the lanthanides, had higher EF values (>10) in all size-resolved
11 particles than La, Pr, Nd, and Sm, demonstrating that Ce is highly influenced by
12 anthropogenic emissions. For the three size-resolved particles, Ce is highly correlated
13 not only with La, Pr, Nd, and Sm but also with a number of anthropogenic elements,
14 again implying that Ce originated from traffic emissions such as automotive catalyst
15 and fuel additive of diesel vehicles as well as from a crustal source (Kulkarni et al.,
16 2006; Cassee et al., 2011).

17 High EFs (> 10) were obtained for As, Ba, Cd, Cu, Cr, Ga, Mo, Sb, Se, and Sn,
18 indicating their anthropogenic origins. Among these elements, Cu is an additive in
19 high temperature lubricant and is present in brake linings, approximately 1 - 10 % by
20 weight (Sanders et al., 2003), and it has been used successfully as a good tracer for
21 wear emission of road traffic (Pio et al., 2013). Correlation analyses (Table 2)
22 illustrate that Ba, Cd, Ga, Mo, Sb, and Sn are well correlated with Cu ($r > 0.93$) in
23 both coarse and fine modes, suggesting that, similar to Cu, these elements in
24 Hsuehshan Tunnel originated mainly from wear abrasive sources. This could be
25 supported by the presence of both BaSO_4 and Sb_2S_3 -containing particles in both brake

1 lining materials, in which the former is utilized as a filler and the latter is utilized as
2 an alternative to asbestos (Ingo et al., 2004). Moreover, the use of organic Sb
3 compounds in grease and motor oil is another road traffic emission source of Sb
4 (Huang et al., 1994; Cal-Prieto, 2001).

5 Lead (Pb) and Zn show high enrichment in all size fractions, indicating that both
6 elements are contributed primarily by traffic emissions, rather than a natural origin.
7 According to the bimodal distribution (Figure 2) and the good correlations with Cu,
8 Ba, and Sb ($r > 0.63$) in $PM_{1.8-10}$ (Table 2), Zn appears to originate from traffic
9 emissions, and two traffic sources could account for the observed Zn. For the coarse
10 mode, Zn is associated with wear tire debris because Zn is added to tires during
11 vulcanization and is responsible for 1 - 2 % of the tires by weight (Degaffe and Tuner
12 2011; Taheri et al., 2011). This is in concert with previous results (Adachi and
13 Tainosho, 2004; Councill et al., 2004; Tanner et al., 2008, Harrison et al., 2012). For
14 the fine mode, Zn is probably contributed by lubrication oil via pipe emissions
15 (Huang et al., 1994). Emissions from vehicle exhaust and wear abrasion are both
16 important sources of Pb. **However, Pb showed good correlation with Cu, Sb, Ba and
17 Zn ($r > 0.60$) in both coarse and fine PM (in Table 2), indicating mixed sources of
18 wear abrasions and pipe emissions. On the contrary, Pb only correlated well with Zn
19 ($r = 0.77$) in submicron size (in Table S3), reflecting that Pb was preferentially
20 contributed by combustion process from vehicle fleets (Wang et al., 2003).**

21 Iron (Fe), which is considered an important crustal element, exhibited enrichment
22 factors of 5 to 11 at the entrance and 12 to 21 at the exit, indicating that Fe in the
23 tunnel was mainly produced from anthropogenic emissions other than road dust.
24 Previous studies have pointed out that in addition to road dust, wear debris from brake
25 linings and tires as well as diesel engine emissions are main sources of Fe in areas

1 near traffic emissions (Cadle et al., 1997; Garg et al., 2000; Wang et al., 2003). In the
2 present study, Fe correlated well with Cu, Ba, and Sb in all sizes ($r > 0.87$, Tables 2
3 and S3), demonstrating that wear dust is a major anthropogenic source of Fe in
4 Hsuehshan Tunnel, as is the case for those elements.

5 PCA results are presented in Table 3, in which the data (samples) are divided into
6 three size groups. Two possible sources are identified for coarse PM. As seen, PC1
7 was associated with Fe, Ba, Mn, Cu, Mo, Cd, Sb and Ga; moderate loadings were
8 found for Zn and Pb. Zinc and Pb are commonly used as lubricating oil in diesel
9 engines. Agarwal et al. (2014) reported that Zn and Pb were detected together and
10 they constituted up to 0.2 % of the total fresh diesel PM, which is consistent with that
11 reported by Sharma et al. (2005); therefore PC1 was likely contributed by wear debris
12 and diesel emissions. High loadings were found for Na, Mg, K, Ca and Rb in PC2,
13 inferring road dust origins. Note that PC2 was also attributed to high loading of Pb.
14 Lead was a crucial additive in gasoline that allowed engine compression to be raised
15 substantially, which in turn increased vehicle performance. Although leaded gasoline
16 has been progressively phased out in mid-1970s, Pb (~0.2% of total mass) has been
17 detected in exhausted PM from gasoline engines (Agarwal et al., 2014). This may
18 support that high loading of Pb in PC2 was attributed to gasoline emissions; as a
19 result, PC2 in coarse mode is likely a mixed source of road dust and gasoline exhaust.
20 For fine particles, Fe, Ba, Mn, Cu, Mo, Cd, Sb, Mg, K, Ca, Rb, La, and Ce all had
21 high loadings, whereas Pb had moderate loadings in PC1; brake abrasion mixed with
22 re-suspended dust and gasoline emissions might explain this factor. In PC2, high
23 positive loading was found for Zn; moderate loading for Pb; thus, PC2 could be
24 explained by diesel emissions. The third component was identified as road dust
25 because of the correlations among Na, Al, and Mg (loadings > 0.6). For submicron

1 particles, high loadings were found for Fe, Ba, Cu, Mo, Sb, Ga and Ce in PC 1. As
2 previously mentioned, Ce in smaller PM may be associated with catalyst converter
3 and fuel additives; therefore, PC 1 might be grouped into mixed sources of wear
4 abrasion and auto catalyst. In PC 2, high positive loadings were found for Pb and Zn,
5 illustrating that exhaust from diesel engine was a potential source in this component.
6 However, PC 3, which had a high loading of Al and a moderate loading of Ca
7 indicates that road dust could be the potential source. **PC4 is a component with high**
8 **loading for V and Ni. Previous studies have suggested that V and Ni in submicron**
9 **particles were commonly attributed to fuel oil combustion of gasoline and diesel**
10 **engines (Wang et al., 2003; Shafer et al., 2008), but higher emission rates for gasoline**
11 **exhaust compared to diesel engines (Cheng et al., 2010b). Consequently, PC4 in**
12 **submicron PM may be associated preferentially from gasoline engines. Overall, wear**
13 **abrasion dust, road rust and combustion process from vehicle fleets are important**
14 **sources of many airborne metals over all size ranges inside Hsuehshan Tunnel.**

15

16 **3.4 Fingerprinting ratios of traffic-derived metals**

17 Cu is used as an indicator for wear debris, and the ratios of wear-derived
18 elements to Cu obtained by linear regression approach can be applied to determine
19 the contribution of specific metals from wear debris in urban atmosphere. Figure 4
20 presents the scatter plots of Fe, Ba, Sb, Sn, Ga and Mo against Cu in PM₁, PM_{1-1.8},
21 and PM_{1.8-10} at the two sites. These elements had strong correlations ($r > 0.9$), and
22 these ratios were constant in different size-resolved PM, strongly suggesting that
23 these ratios can be applied as good fingerprinting ratios of wear emissions. The
24 mean mass ratios of Fe/Cu, Ba/Cu, Sb/Cu, Sn/Cu, and Ga/Cu were 14, 1.05, 0.16,
25 0.10 and 0.03, respectively. Table 4 compares our ratios to those established by other

1 tunnel studies. The ratios of Fe/Cu held around 14 to 15 over all sizes in the present
2 work, which agrees with that (14) acquired by dynamometer tests (Sanders et al.,
3 2003) and is also comparable to those observed in different tunnels (Gillies et al.,
4 2001; Fabretti et al., 2009; Cheng et al., 2010b; Pio et al., 2013). However, the
5 Fe/Cu ratio is also significantly distinct from those (37 to 60) found in other tunnels;
6 such difference may have arisen from discrepancies in ingredients of brake pads and
7 in driving conditions (Garg et al., 2000). Ba/Cu ratios of 0.8 - 1.1 were similar to
8 those found in Europe but slightly lower than that (> 2) found in the United States.
9 Our Sb/Cu ratio of 0.16 is consistent with the result obtained in Hong Kong but
10 lower than that (0.76 to 0.88) occasionally measured in American countries (Gillies
11 et al., 2001; Mancilla and Menodza, 2012). In Japan, Iijima et al. (2007), with the
12 use of dynamometer tests, reported Sb/Cu ratios ranging from 0.05 to 0.11 for
13 different brake pads. They also pointed out that Sb-free brake pads have been
14 utilized recently in Japanese passenger cars. According to the Taiwan Transportation
15 Vehicle Manufactures Association 44 % and 13 % of vehicle fleets in Taiwan are
16 Japanese and American cars, respectively. The abundance of Japanese cars in Taiwan
17 may have caused the lower Sb/Cu values in this work. For the Mo against Cu scatter
18 plot, two slopes are obtained: 0.05 for coarse and fine particles and 0.12 for particles
19 with aerodynamic diameter less than $0.56 \mu\text{m}$. The enhancement of Mo in such
20 submicron particles is perhaps attributed to an additional source of Mo such as
21 diesel exhausts (Kuo et al., 2009). Previous studies show that the ratio of V/Ni has
22 been widely used as a fingerprinting ratio of specific anthropogenic origins. For
23 example, heavy oil combustion shows a narrow range of V/Ni ratio (3 to 4)
24 (Hedberg et al., 2005; Mazzei et al., 2008). Combustion origins from gasoline and
25 diesel vehicles have smaller V/Ni ratios (< 2.0) (Qin et al., 1997; Watson et al.,

1 2001). On the other hand, small quantities of V and Ni are also found in soil with a
2 V/Ni ratio of < 1.5 (Hsu et al., unpublished data). In this work, V/Ni ratios were
3 typically lower than 2.0 in fine and submicron PM; the ratios which were
4 alternatively acquired directly from their mass concentrations (instead of linear
5 regression) because V is not strongly correlated with Ni ($r < 0.5$, Tables 2 and S3) in
6 three different sizes. In fine and submicron PM, the lower V/Ni ratios with higher
7 EF value (>10) for both elements suggest that they were contributed mostly by oil
8 combustion from traffic fleets. In coarse PM, a low V/Ni ratio (<2) and a low EF
9 value (~ 2) for V indicate that V was associated with soil origins; however, high EF
10 for Ni suggests that Ni was contributed by combustion sources. The Pb/Cu ratios in
11 the tunnel particles averaged at 0.07, which is much lower than those (much higher
12 than unity) usually observed in ambient air (Fang et al., 2005). In addition, the
13 tunnel particles had As/Sb and Se/Sb ratios of 0.1 and 0.05, respectively, which are
14 also evidently lower than those (around unity) measured in ambient aerosols (Querol
15 et al., 2007). These results imply that traffic emissions are not major sources of Pb,
16 As, and Se in ambient atmospheres.

17 **Figure 5** illustrates the relationships of La against Ce, Pr, Nd, and Sm. Their
18 correlations weaken with decreasing particle size, suggesting that the REEs in
19 smaller particles were disturbed by certain anthropogenic sources. A ratio of La/Ce
20 has been successfully used to distinguish natural sources from anthropogenic origins
21 (Kulkarni et al., 2006). In this work, the La/Ce ratios that range from 0.15 to 0.18
22 and from 0.10 to 0.12 at the inlet and outlet sites, respectively, are expectedly
23 significantly lower than that of average crust (~ 0.50) (Taylor, 1964) and soils (~ 0.7)
24 (Kulkarni et al., 2006). Such values agree with those of Kulkarnu et al. (2006) and
25 Huang et al. (1994) who reported that La/Ce ratios for traffic emissions were 0.20

1 and 0.13, respectively. As discussed in Section 3.2, the EF values of Ce were mostly
2 higher than unity at both the inlet and outlet sites, with even some of the values
3 being one order of magnitude higher (Figure 3), revealing that soil dust is not the
4 sole source of Ce. Thus, the low La/Ce values found in the present study could be
5 attributed to an additional supply of Ce from vehicular emissions.

6

7 **4. Summary and concluding remarks**

8 Size-fractionated aerosol samples were collected in Hsuehshan Tunnel to
9 characterize particulate metals emitted by vehicle fleets. A total of 36 elements were
10 analyzed by ICP-MS. Compared to the entrance, enhanced concentrations for most
11 metals at the exit are due to “piston effect”. With regard to enrichment factor,
12 correlation matrix, and principal component analysis, the analyzed metals were
13 categorized into three groups, namely, wear abrasion (Cu, Cd, Cu, Fe, Ga, Mn, Mo,
14 Sb, and Sn), re-suspended dust (Ca, Mg, K and Rb), and pipe emissions (Zn, Pb and
15 V). Size distributions of these elements were significantly different because of their
16 origins. For wear-related metals and geological elements, a mono-modal size
17 distribution was found and the major peak shifted from the range of 3.2 - 5.6 μm at
18 the entrance to the range of 1 - 1.8 μm at the exit. However, elements attributed to
19 combustion sources were predominant mainly in submicron particles and peaked at
20 0.56 - 1.0 μm at the inlet site and at 0.18 - 0.32 μm or 0.32 - 0.56 μm at the outlet
21 site. By adopting Cu as an indicator element of wear debris, fingerprinting ratios
22 were constructed, including Fe/Cu, Ba/Cu, Sb/Cu, Sn/Cu and Ga/Cu. These ratios
23 can effectively apportion the source of specific elements in urban environment from
24 wear abrasion.

25 **In this work, we characterized traffic-derived PM metals using a tunnel study.**

1 The data would be useful for future studies on traffic emission inventory and health
2 effects, especially for submicron PM. Wear abrasion appeared to be a major source
3 of specific toxic elements. While the government focuses on exhaust emission
4 control, the contribution of wear from brake linings and tires could not be ignored.
5 Thus, stringent implementations of measures for reducing wear emissions are
6 needed in the future.

7

8 **Acknowledgements**

9 This project is part of the “Development of Analytical Tools for Measuring and
10 Characterizing Nanomaterials in the Environment” (EPA-101-1602-02-08 and
11 EPA-102-1602-02-01) and was financially supported by the Environmental Analysis
12 Laboratory of the Environmental Protection Administration in Taiwan. We would
13 like to thank the Directorate General of Highways, MOTC, Taiwan, for supporting
14 the sampling collection in Hsuehshan Tunnel and for providing related information.

15

16 **References**

- 17 Abu-Allaban, M., Coulomb, W., Gertler, A. W., Gillies, J., Pierson, W. R., Rogers,
18 C. F., Sagebiel, J. C., and Tarnay, L.: Exhaust particle size distribution
19 measurements at the Tuscarora Mountain Tunnel. *Aerosol Sci. Technol.*, 36,
20 771-789, doi:10.1080/02786820290038401, 2002.
- 21 Adachi, K., and Tainosho, Y.: Characterization of heavy metal particles embedded
22 in the tire dust, *Environ. Int.*, 30, 1009-1017, doi:10.1016/j.envint.2004.04.004,
23 2004.
- 24 Agarwal, A. K., Gupta, T., Bothra, P., Shukla, P. C.: Emissions profiling of diesel
25 and gasoline cars at a city traffic junction, *Particuology*, in press,

1 [doi:10.1016/j.partic.2014.06.008](https://doi.org/10.1016/j.partic.2014.06.008),2014

2 Amato, F., Karanasiou, K., Moreno, T., Alastuey, A., Orza, J. A. G., Lumbreras, J.,
3 Borge, R., Boldo, E., Linares, C., and Querol, X.: Emission factors from road
4 dust resuspension in a Mediterranean freeway, *Atmos. Environ.*, 61, 580-587,
5 doi:10.1016/j.atmosenv.2012.07.065, 2012.

6 Birmili, W., Allen, A. G., Bary, F., and Harrison, R.M.: Trace metal concentrations
7 and water solubility in size-fractionated atmospheric particles and influence of
8 road traffic, *Environ. Sci. Technol.*, 40, 1144-1153, doi:10.1021/es0486925,
9 2006.

10 Brauer, M., Hoek, G., Vliet, V. P., Meliefste, K., Fischer, P. H., Wijga, A.,
11 Koopman, L. P., Neijens, H. J., Gerritsen, J., Kerkhof, M., Heinrich, J.,
12 Bellander, T., and Brunekreef, B.: Air pollution from traffic and the development
13 of respiratory infections and asthmatic and allergic symptoms in children, *Am. J.*
14 *Respir. Crit. Care Med.*, 166, 1092-1098, doi:10.1164/rccm.200108-007OC,
15 2002.

16 Brito, J., Rizzo, L. V., Herckes, P., Vasconcellos, P. C., Caumo, S. E. S., Fornaro, A.,
17 Ynoue, R. Y., Artaxo, P., and Andrade, M. F., Physical-chemical
18 characterisation of the particulate matter inside two road tunnels in the São Paulo
19 metropolitan Area, *Atmos. Chem. Phys.*, 13, 12199-12213,
20 doi:10.5194/acp-13-12199-2013, 2013.

21 Cadle, S. H., Mulawa, P. A., Ball, J., Donase, C., Weibel, A., Sagebiel, J. C., Knapp,
22 K. T., and Snow, R.: Particulate emission rates from in use high emitting
23 vehicles recruited in Orange County, California, *Environ. Sci. Technol.*, 31,
24 3405-3412, doi:10.1021/es9700257, 1997.

25 Cadle, S. H., Mulawa, P. A., Hunsanger E.C., Nelson, K., Ragazzi, R. A., Barrett, R.,

1 Gallagher, G. L., Lawson, D. R., Knapp, K. T., and Snow, R.: Composition of
2 light-duty motor vehicle exhaust particulate matter in the Denver, Colorado area,
3 Environ. Sci. Technol., 33, 2328-2339, doi:10.1021/es9810843, 1999.

4 Cal-Prieto, M. J., Carlosena, A., Andrade, J. M., Martinez, M. L., Muniategui, S.,
5 Lopez-Mahia, P., and Prada, D.: Antimony as a tracer of the anthropogenic
6 influence on soil and estuarine sediments, Water, Air, and Soil Pollut., 129,
7 333-348, doi:10.1023/A:1010360518054, 2001.

8 Cassee, F. R., van Balen, E. C., Singh, C., Green, D., Muijsers, H., Weinstein, J., and
9 Dreherk, K.: Exposure, health and ecological effects review of engineered
10 nanoscale cerium and cerium oxide associated with its use as a fuel additive. Crit.
11 Rev. Toxicol., 41, 213-229, doi:10.3109/10408444.2010.529105, 2011.

12 Chang, S.-C., Lin, T.-H., and Lee, C.-T.: On-road emission factors from light-duty
13 vehicles measured in Hsuehshan Tunnel (12.9 km), the longest tunnel in Asia,
14 Environ. Monit. Assess., 153, 187-200, doi:10.1007/s10661-008-0348-9, 2009.

15 Chen, S.-C., Tsai, C. J., Chou, Charles C.-K., Roam, G.-D., Cheng, S.-S., and Wang,
16 Y.-N.: Ultrafine particles at three different sampling locations in Taiwan. Atmos.
17 Environ., 44, 553-540, doi:10.1016/j.atmosenv.2009.10.044, 2010.

18 Cheng, Y.-H., Liu, Z.-S., and Chen, C.-C.: On-road measurements of ultrafine
19 particle concentration profiles and their size distributions inside the longest
20 highway tunnel in Southeast Asia, Atmos. Environ., 44, 763-772,
21 doi:10.1016/j.atmosenv.2009.11.40, 2010a.

22 Cheng, Y., Lee, S. C., Ho, K. F., Chow, J. C., Watson, J. G., Louie, P. K. K., Cao, J.
23 J., and Hai, X.: Chemically-specified on road PM_{2.5} motor vehicle emission
24 factors in Hong Kong. Sci. Total. Environ., 408, 1621-1627,
25 doi:10.1016/j.scitotenv.2009.11.061, 2010b.

1 Chiang, H.-L., and Huang, Y.-S.: Particulate matter emissions from on-road vehicles
2 in a freeway tunnel study, *Atmos. Environ.*, 43, 4014-4022,
3 doi:10.1016/j.atmosenv.2009.05.015, 2009.

4 Councill, T. B., Duckenfield K. U., Landa, E. R., and Callender, E.: Tire-wear
5 particles as a source of Zn to the environment, *Environ. Sci. Technol.*, 38,
6 4206-4214, doi:10.1021/es034631f, 2004.

7 Dall'Osto, M., Querol, X., Amato, F., Karanasiou, A., Lucarelli, F., Nava, S., Calzolari,
8 G., and Chiari, M.: Hourly elemental concentrations in PM_{2.5} aerosols sampled
9 simultaneously at urban background and road site during SAPUSS-diurnal
10 variations and PMF receptor modeling, *Atmos. Chem. Phys.*, 13, 4375-4392,
11 doi:10.5194/acp-13-4375-2013, 2013.

12 Defino, R. J., Siotuas, C., and Malik, S.: Potential role of ultrafine particles in
13 associations between airborne particle mass and cardiovascular health, *Environ.*
14 *Health Perspect.*, 113, 934-938, doi:10.1289/ehp.7938, 2005.

15 Degaffe, F. S., and Turner, A.: Leaching of zinc from tire wear particles under
16 simulated estuarine conditions, *Chemosphere*, 85, 738-743,
17 doi:10.1016/j.chemosphere.2011.06.047, 2011.

18 Fabretti, J.-F., Sauret, N., Gal, J.-F., Maria, P.-C., and Schärer, U.: Elemental
19 characterization and sources identification of PM_{2.5} using Positive Matrix
20 Factorization: the Malraux road tunnel, Nice, France, *Atmos. Res.*, 94, 320-329,
21 doi:10.1016/j.atmosres.2009.06.10, 2009.

22 Fang G.-C., Wu, Y.-S., Huang, S.-H., and Rau, J.-Y.: Review of atmospheric
23 metallic elements in Asia during 2000–2004, *Atmos. Environ.*, 39, 3003–3013,
24 doi:10.1016/j.atmosenc.2005.01.042, 2005.

25 Funasaka, K., Miyazaki, T., Kawaraya, T., Tsuruho, K., and Mizuno, T.:

1 Characteristics of particulates and gaseous pollutants in a highway tunnel,
2 Environ. Pollut.,102, 171-176, doi:10.1016/S0269-7491(98)00101-8, 1998.

3 Garg, B. D., Cadle, S. H., Mulawa, P. A., Groblicki, P. J., Laroo, C., and Parr, G. A.:
4 Brake wear particulate matter emissions, Environ. Sci. Technol., 34, 4463-4469,
5 doi:10.1021/es001108h, 2000.

6 Gillies, J. A., Gertler, A. W., Sagebiel, J. C., and Dippel, W. A.: On-road particulate
7 matter (PM_{2.5} and PM₁₀) emissions in the Sepulveda tunnel, Los Angeles,
8 California, Environ. Sci. Technol., 35, 1054-1063, doi:10.1021/es991320p, 2001.

9 Grieshop, A. P., Lipsky, E. M., Pekney, N. J., Takahama, S., and Robinson, A. L.:
10 Fine particle emission factors from vehicle in a highway tunnel: effects of fleet
11 composition and season, Atmos. Environ., 40, 287-298,
12 doi:10.1016/j.atmosenv.2006.03.064, 2006.

13 Handler, M., Puls, C., Zbiral, J., Marr, I., Puxbaum, H., and Limbeck, A.: Size and
14 composition of particulate emissions from motor vehicles in the
15 Kaisermühlen-Tunnel, Atmos. Environ., 42, 2173-2186, doi:10.1016/j.stmosenv.
16 2007.11.054, 2008.

17 Harrison, R. M., Jones A. M., Gielt, J., Yin, J., and Green, D. C.: Estimation of the
18 contributions of brake dust, tire wear, and resuspension to nonexhaust traffic
19 particles derived from atmospheric measurements. Environ. Sci. Technol., 46,
20 6523-6529, doi:10.1021/es300894r, 2012.

21 He, L.Y.; Hu, M.; Zhang, Y.H.; Huang, X.F.; Yao, T.T. Fine particle emissions from
22 on-road vehicles in the Zhujiang tunnel, China, Environ. Sci. Technol.,
23 42, 4461-4466, doi:10.1021/es7022658, 2008.

24 Hedberg, E., Gidhagen, L., Johansson, C.: Source contributions to PM₁₀ and arsenic
25 concentrations in Central Chile using positive matrix factorization, Atmo.

1 Environ., 39, 549-561, doi:10.1016/j.atmosenv.2004.11.001, 2005.

2 Hee, K. W., and Filip, P.: Performance ceramic enhanced phenolic matrix brake
3 linings materials for automotive brake linings, *Wear*, 29, 1088-1096,
4 doi:10.1016/j.wear.2005.02.083, 2005.

5 Hsu, S.-C., Liu, S. C., Huang, Y. T., Lung, S.-C. Candice, Tsai, F., Tu, C.-Y., and
6 Kao, S.-J.: A criterion for identifying Asian dust events based on Al concentration
7 data collected from northern Taiwan between 2002 to early 2007, *J. Geophys. Res.*,
8 113, doi:10.1029/2007JD009574, 2008.

9 Hsu, S.-C., Liu, S. C., Huang, Y.-T., Chou, Charles, C. K., Lung, S. S. Candice, Liu,
10 T. H., Tu, J.-Y., and Tsai, F.: Long-range southeastward transport of Asian
11 biomass pollution: Signature detected by aerosol potassium in Northern Taiwan,
12 *J. Geophys. Res.*, 114, doi:10.1029/2009JD011725, 2009.

13 Hsu, S. C., Liu, S. C., Tsai, F., Engling, G., Lin, I. I., Chou, C. K. C., Kao, S. J., Lung,
14 S. C. C., Chan, C. Y., Lin, S. C., Huang, J. C., Chi, K. H., Chen, W. N., Lin, F. J.,
15 Huang, C. H., Kuo, C. L., Wu, T. C., and Huang, Y. T.: High wintertime
16 particulate matter pollution over a offshore island (Kinmen) off Southeastern
17 China: an overview, *J. Geophys. Res.*, 115, D17309, doi:10.1029/2009JD013641,
18 2010.

19 Huang, X., Olmez, I., Aras, N. K., and Gordon, G. E.: Emissions of trace elements
20 from motor vehicles: potential marker elements and source composition profile,
21 *Atmos. Environ.*, 28, 1385-1391, doi:10.1016/1352-2310(94)90201-1, 1994..

22 Iijima, A., Sato, K., Yano, K., Tago, H., Kato, M., Kimura, H., and Furuta, N.:
23 Particle size and composition distribution analysis of automotive brake abrasion
24 dusts for the evaluation of antimony sources of airborne particulate matter. *Atmos.*
25 *Environ.*, 41, 4908-4919, doi:10.1016/j.atmosenv.2007.02.005, 2007.

- 1 Ingo, G. M., D'Uffizi, M., Falso, G., Bultrini, G., and Padeletti, G.: Thermal and
2 microchemical investigation of automotive brake pad wear residues, *Thermochim*
3 *Acta.*, 418, 61-68, doi:10.1016/j.tca.2003.11.042, 2004.
- 4 Jamriska, M., Morawska, L., Thomas, S., and He, C.: Diesel bus emissions measured
5 in a tunnel study. *Environ. Sci. Technol.*, 38, 6701-6709, doi:10.1021/es030662z,
6 2004.
- 7 Johansson, C., Norman, M., and Burman, L.: Road traffic emission factors for heavy
8 metals, *Atmos. Environ.*, 43, 4681-4688, doi:10.1016/j.atmosenv. 2008. 10.1024,
9 2009.
- 10 Kulkarni, P., Chellam, S., and Fraser, M. P.: Lanthanum and lanthanides in
11 atmospheric fine particles and their apportionment to refinery and petrochemical
12 operations in Houston, TX, *Atmos. Environ.*, 40, 508-520,
13 doi:10.1016/j.atmosenv.2005.09.063, 2006.
- 14 Kuo, C.-Y., Wang, J.-Y., Chang, S.-H., and Chen, M.-C.: Study of metal
15 concentrations in the environment near diesel transport routes, *Atmos. Environ.*,
16 43, 3070-3076, doi:10.1016/j.atmosenv. 2009.03.028, 2009.
- 17 Lai, C.-H., and Peng, Y.-P.: Volatile hydrocarbon emissions from vehicles and
18 vertical ventilations in the Hsuehshan traffic tunnel, Taiwan, *Environ. Monit.*
19 *Assess.*, 184, 4015-4028, doi:10.1007/s10661-011-2240-2, 2012.
- 20 Lawrence, S., Sokhi, R., Ravindra, K, Mao, H., Prain, H. D., and Bull, I. D.: Source
21 apportionment of traffic emissions o particulate matter using tunnel measurements,
22 *Atmos. Environ.*, 77, 548-557, doi:10.1016/j.atmosenv.2013.03.040, 2013
- 23 Li, H.-C., Chen, K.S., Lai, C-H., and Wang, H.-K.: Measurements of gaseous
24 pollutant concentrations in the Hsuehshan traffic tunnel of Northern Taiwan,
25 *Aerosol Air Qual. Res.*, 11, 776-782, doi:10.4209/aaqr.2011.02.0009, 2011.

1 Lin, C.-C., Chen, S.-J., Huang, K.-L., Hwang, W.-I., Chang-Chien, G. P., and Lin,
2 W. Y.: Characteristics of metals in nano/ultrafine/fine/coarse particles collected
3 beside a heavily trafficked road, *Environ. Sci. Technol.*, 39, 8113-8125, doi:
4 10.1021/es048182a, 2005.

5 Lough, G. C., Schauer, J. J., Park, J.-S., Shafer, M. M., Deminter, J. T., and
6 Weinstein, J. P.: Emissions of metal associated with motor vehicle roadways,
7 *Environ., Sci. Technol.*, 39, 826-836, doi:10.1021/es048715f. 2005.

8 Mancilla, Y., and Mendoza, A.: A tunnel study to characterize PM_{2.5} emissions from
9 gasoline-powered vehicles in Monterrey, Mexico. *Atmos. Environ.*, 59, 449-460,
10 doi: :10.1016/j.atmosenv.2012.05.025, 2012.

11 Mazzei, F., D'Alessandro, A., Lucarelli, F., Nava, S., Prati, P., Valli, G., and Vecchi,
12 R.: Characterization of particulate matter sources in an urban environment, *Sci*
13 *Total Environ.*, 401, 81-89, doi:10.1016/j.scitotenv.2008.03.008, 2008.

14 Moreno, T., Pérez, N., Reche, C., Martins, C., de Miguel, E., Capdevila, M., Centelles,
15 S., Minguillón, M. C., Amato, F., Alastuey, A., Querol, X., and Gibbson, W.:
16 Subway platform air quality: assessing the influences of tunnel ventilation, train
17 piston effect and station design, *Atmos. Environ.*,
18 doi:10.1016/j.atmosenv.2014.04.043, 2014.

19 Nel, A.: Air pollution-related illness: effects of particle, *Science*, 308, 804-806,
20 doi:10.1126/science1108752, 2005.

21 Ning, Z., Polidori, A., Schauer, J. J. Sioutas, C.: Emission factors of PM species
22 based on freeway measurements and comparison with tunnel and dynamometer
23 studies, *Atmos. Environ.*, 42, 3099-3114. doi:10.1016/j.atmosenv.2007.12.039,
24 2007.

25 Ntziachristos, L., Ning, Z., Geller, M.D., Sioutas, C.: Particle concentration and

1 characteristics near a major freeway with heavy-duty diesel traffic. *Environ. Sci.*
2 *Technol.*, 41, 2223-2230. doi:10.1021/es062590s, 2007.

3 Pio, C., Mirante, F., Oliveira, C., Matos, M., Caseiro, A., Oliveira, C., Querol, X.,
4 Alves, C., Martins, N., Cerqueira, M., Camões, F., Silva, H., and Plana, F.:
5 Size-segregated chemical composition of aerosol emissions in an urban road
6 tunnel in Portugal, *Atmos. Environ.*, 71, 15-25,
7 doi:10.1016/j.atmosenv.2013.01.037, 2013.

8 Qin, Y., Chan, K. C., and Chan, Y. L.: Characteristics of chemical compositions of
9 atmospheric aerosol in Hong Kong, spatial and seasonal distributions, *Sci. Total*
10 *Environ.*, 206, 25-37, doi:10.1016/S00489697(97)00214-3, 1997.

11 Querol, X., Viana, M., Alastuey, A., Amato, F., Moreno, T., Castillo, S., Pey, J., de la
12 Rosa, J., Sánchez de la Campa A., Artíñano, B., Salvador, P., García Dos Santos
13 S., Fernández-Patier R., Moreno-Grau, S., Negral, L., Minguillón, M. C.,
14 Monfort E., Gil, J. I., Inza, A., Ortega, L. A., Santamaría, J. M., and Zabalza, J.:
15 Source origin of trace elements in PM from regional background, urban and
16 industrial sites of Spain, *Atmos. Environ.*, 41, 7219–7231,
17 doi:10.1016/j.atmos.env.2007.05.022.

18 Rogge, W. F., Hildemann, L. M., Mazurek, M. A., Cass, G. R., and Simoneit, B. R. T.:
19 Sources of fine organic aerosol. 3. Road dust, tire debris, and organometallic brake
20 lining dust-roads as source and sinks, *Environ. Sci. Technol.*, 27, 1892-1904,
21 doi:10.1021/es00046a019, 1993.

22 Sanders, P. G., Xu, N., Dalka, T. M., and Maricq, M. M.: Airborne brake wear debris:
23 size distributions, composition, and a comparison of dynamometer and vehicle
24 tests, *Environ. Sci. Technol.*, 37, 4060-4069, doi:10.1021/es034145s, 2003.

25 Shafer, M. M., Toner, B. M., Overdier, J. T., Schauer, J. J., Fakra, S. C., Hu, S.,

1 Herner, J. D., and Ayala, A.: Chemical speciation of vanadium in particulate
2 matter emitted from diesel vehicles and urban atmospheric aerosols, *Environ. Sci.*
3 *Technol.*, 46, 189-195, doi:10.1021/es200463c, 2012.

4 Sharma, M., Agarwal, A. K., Bharathi, K. V. L.: Chracterization of exhaust
5 particulates from diesel engine. *Atmos. Environ.*, 39, 3023-3028,
6 doi:10.1016/j.atmosenv.2004.1.047, 2005.

7 Sternbeck, J., Sjödin, Å., and Andréasson, K.: Metal emissions from road traffic and
8 the influence of resuspension-results from two tunnel studies, *Atmos. Environ.*,
9 36, 4735-4744, doi:10.1016/S1352-2310(02)00561-7, 2002.

10 Taheri, S., Khoshgoftarmanesh, A. H., Shariatmadari, H., Chaney, R. L.: Kinetics of
11 zinc release from ground tire rubber and rubber ash in a calcareous soil as
12 alternatives to Zn fertilizers. *Plant Soil*, 341, 89-91,
13 doi:10.1007/s11104-010-0624-7, 2011.

14 Thorp, A., and Harrison, R. M.: Sources and properties of non-exhaust particulate
15 matter from road traffic: a review, *Sci. Total Environ.*, 400, 270-282,
16 doi:10.1016/j.scitotenc.2008.06.007, 2008.

17 Tanner, P. A., Hoi-Ling, M., and Yu, P. K. N.: Fingerpriting metals in urban street
18 dust in Beijing, Shanghai and Hong Kong, *Environ. Sci. Technol.*, 42, 7111-7117,
19 doi:10.1021/es8007613, 2008.

20 Taylor, S. R.: Abundance of chemical elements in the continental crust: a new table.
21 *Grochim. Cosmochim. Acta.*, 18, 1273-1285, doi:10.1016/0016-7037(64)90129-2,
22 1964.

23 Wåhlin, P., Berkowicz, R., and Palmgren F.: Characterization of traffic-generated
24 particulate matter in Copenhagen, *Atmos. Environ.*, 40, 2151-2159,
25 doi:10.1016/j.atmosenv.2005.11.049, 2006.

- 1 Wang, Y.-F., Huang, K.-L., Li, C.-T., Mi, H.-H., Luo, J.-H., and Tsai, P.-J.:
2 Emissions of fuel metals content from a diesel vehicle engine, *Atmos. Environ.*, 33,
3 4637-4643, doi:10.1016/j.atmosenv.2003.07.007, 2003.
- 4 Watson, J., Chow, J., and Houck, J. E.: PM_{2.5} chemical source profiles for vehicle
5 exhaust, vegetative burning, geological material and coal burning in Northwestern
6 Colorado during 1995, *Chemosphere*, 43, 1141-1151,
7 doi:10.1016/S00456535(00)00171-5, 2001.
- 8 Weingartner, E., Keller, C., Stahel, W. A., Burtscher, H., and Baltensperger, U.:
9 Aerosol emission in a road tunnel, *Atmos. Environ.*, 31, 451-462,
10 doi:10.1016/S1352-2310(96)00193-8, 1997.
- 11 Zhang, R., Jing, J., Tao, J., Hsu, S.-C., Wang, G., Cao, J., Lee, C. S. L., Zhu, L.,
12 Chen, Z., Zhao, Z., and Shen, Z.: Chemical characterization and source
13 apportionment of PM_{2.5} in Beijing: seasonal perspective, *Atmos. Chem. Phys.*,
14 13, 7053-7074, doi:10.5194/acp-13-7053-2013, 2013.
- 15 Zhu, C.-S., Chen, C.-C., Cao, J.-J., Tsai, C.-J., Chou, Charles, C.-K., Liu, S.-C., and
16 Roam, G.-D.: Characterization of carbon fractions for atmospheric fine particles
17 and nonparticles in a highway tunnel, *Atmos. Environ.*, 44, 2668-2673,
18 doi:10.1016/j.atmosenv.2010.04.042, 2010.

Table captions

Table 1. Summary of sampling dates, mass concentrations ($\mu\text{g}/\text{m}^3$) of $\text{PM}_{1.8-10}$, $\text{PM}_{1-1.8}$ and PM_1 as well as traffic flow and wind speed in Hsuehshan Tunnel during the sampling periods in 2013.

Table 2. Correlation matrix of selected elements in coarse (top side triangle) and fine particles (lower side triangle) observed in Hsuehshan Tunnel. Correlation coefficients higher than 0.8 are marked in bold.

Table 3. Summaries of principal component analysis for trace metals in coarse, fine and submicron particles observed in Hsuehshan Tunnel. Factor loadings lower than ± 0.4 are not given. Loading factor greater than 0.7 is marked by bold.

Table 4. Ratios of specific elements to Cu of PM in tunnel PM.

Figure captions

Figure 1. (a) Elemental compositions of PM₁₀ collected at both the inlet and outlet sites in Hsuehshan Tunnel; (b) partitioning of trace metals within three sized PM; (c) outlet-to-inlet ratio for each element in PM₁₀. The sequence of metallic species is in order of decreasing concentrations (ng/m³) at the outlet site. N denotes the number of aerosol samples.

Figure 2. Average size distributions of traffic-derived elements observed at the inlet and outlet sites inside Hsuehshan Tunnel.

Figure 3. Enrichment factors of trace metals in (a) PM₁, (b) PM_{1-1.8} and (c) PM_{1.8-10} observed at the inlet and outlet sites in Hsuehshan Tunnel.

Figure 4. Scatter plots of (a) Fe, (b) Ba, (c) Sb, (d) Sn, (e) Ga, (f) Mo against Cu concentrations (ng/m³) in different size-segregated particles observed in Hsuehshan Tunnel.

Figure 5. Scatter plots of La and (a) Ce, (b) Pr, (c) Nd and (d) Sm concentrations (ng/m³) in different size-segregated particles observed in Hsuehshan Tunnel.

Table 1

Summary of sampling dates, mass concentrations ($\mu\text{g}/\text{m}^3$) of $\text{PM}_{1.8-10}$, $\text{PM}_{1-1.8}$ and PM_1 as well as traffic flow and wind speed in Hsuehshan Tunnel during the sampling periods in 2013.

Sampling No.	Date	Inlet Site			Outlet Site			Vehicle fleet		Wind Speed (m/s)
		$\text{PM}_{1.8-10}$	$\text{PM}_{1-1.8}$ ($\mu\text{g}/\text{m}^3$)	PM_1	$\text{PM}_{1.8-10}$	$\text{PM}_{1-1.8}$ ($\mu\text{g}/\text{m}^3$)	PM_1	LDV (No./hr)	HDV (No./hr)	
1	2013/5/17	17	4	32	17	9	155	1272	72	4.7
2	2013/5/18	18	7	43	18	11	128	1777	88	4.6
3	2013/5/19	19	6	35	21	12	208	1843	109	4.7
4	2013/7/19	16	4	27	26	9	83	1277	104	4.3
5	2013/7/20	16	3	34	15	9	142	1400	118	4.8
6	2013/7/21	13	3	33	20	9	168	1680	126	4.7
7	2013/8/8	17	4	26	15	11	142	1354	109	4.7
8	2013/8/9	19	4	39	9	10	87	1460	133	5.2
9	2013/8/10	9	3	23	16	10	126	1712	81	4.9
10	2013/9/27	27	4	22	28	10	125	1334	81	4.7
11	2013/9/28	22	4	39	16	9	85	1764	101	5.0
12	2013/9/29	15	4	34	18	10	180	1909	121	4.7

Table 2

Correlation matrix of selected elements in coarse (top side triangle) and fine particles (lower side triangle) observed in Hsuehshan Tunnel.

Correlation coefficients higher than 0.8 are marked in bold.

	Al ^a	Fe	Mg	K	Ca	Sr	Ba	Ti	Mn	Ni	Cu	Zn	Mo	Cd	Sn	Sb	Pb	V	Cr	Rb	Cs	Ga	La	Ce	Pr	Nd
Al		0.29	0.42	0.44	0.44	0.45	0.29	0.35	0.34	0.05	0.25	0.43	0.16	0.19	0.17	0.17	0.49	0.20	0.10	0.47	0.41	0.30	0.40	0.20	0.45	0.25
Fe	0.69		0.27	0.31	0.43	0.88	0.97	0.96	1.00	-0.03	0.99	0.66	0.98	0.97	0.97	0.98	0.64	0.74	0.57	0.41	0.38	0.96	0.71	0.91	0.73	0.90
Mg	0.78	0.84		0.74	0.61	0.62	0.36	0.44	0.30	-0.09	0.24	0.31	0.23	0.29	0.29	0.24	0.62	0.42	0.03	0.75	0.62	0.38	0.66	0.44	0.55	0.50
K	0.71	0.89	0.84		0.61	0.63	0.45	0.44	0.36	0.25	0.22	0.56	0.25	0.32	0.31	0.26	0.68	0.45	0.37	0.91	0.88	0.45	0.68	0.48	0.69	0.55
Ca	0.70	0.86	0.82	0.86		0.75	0.57	0.56	0.48	-0.05	0.38	0.59	0.39	0.48	0.47	0.46	0.90	0.49	0.13	0.81	0.74	0.61	0.82	0.47	0.74	0.55
Sr	0.64	0.99	0.86	0.89	0.88		0.94	0.93	0.90	-0.04	0.83	0.76	0.83	0.88	0.87	0.86	0.87	0.75	0.45	0.75	0.67	0.94	0.90	0.86	0.88	0.90
Ba	0.60	0.98	0.81	0.87	0.82	0.99		0.95	0.97	-0.04	0.93	0.77	0.94	0.96	0.96	0.96	0.75	0.73	0.52	0.56	0.52	1.00	0.81	0.91	0.82	0.92
Ti	0.68	0.99	0.85	0.87	0.84	0.98	0.97		0.96	0.02	0.96	0.70	0.95	0.96	0.96	0.96	0.75	0.79	0.50	0.55	0.51	0.95	0.80	0.88	0.75	0.89
Mn	0.63	0.95	0.80	0.90	0.91	0.95	0.95	0.93		0.45	0.98	0.69	0.97	0.96	0.97	0.97	0.68	0.75	0.60	0.46	0.43	0.97	0.74	0.90	0.76	0.90
Ni	0.01	0.08	0.02	0.11	-0.01	0.05	0.06	0.06	0.12		-0.09	-0.02	-0.07	-0.11	-0.10	-0.09	-0.03	-0.02	0.73	0.15	0.16	-0.05	0.05	0.00	0.06	0.03
Cu	0.66	0.99	0.83	0.85	0.82	0.98	0.97	1.00	0.93	0.06		0.63	0.99	0.97	0.98	0.98	0.60	0.73	0.51	0.32	0.30	0.93	0.66	0.87	0.64	0.85
Zn	0.22	0.50	0.34	0.55	0.61	0.50	0.52	0.47	0.72	0.43	0.45		0.63	0.72	0.67	0.67	0.76	0.49	0.31	0.56	0.51	0.78	0.67	0.56	0.65	0.60
Mo	0.61	0.98	0.81	0.84	0.82	0.98	0.98	0.99	0.93	0.05	0.99	0.47		0.98	0.99	0.99	0.60	0.75	0.54	0.34	0.33	0.93	0.67	0.88	0.65	0.86
Cd	0.56	0.96	0.76	0.86	0.87	0.95	0.96	0.95	0.98	0.17	0.95	0.70	0.96		1.00	0.99	0.68	0.73	0.49	0.43	0.41	0.96	0.72	0.87	0.69	0.86
Sn	0.60	0.98	0.80	0.84	0.83	0.98	0.97	0.99	0.93	0.05	0.99	0.48	1.00	0.96		0.99	0.66	0.74	0.51	0.41	0.40	0.95	0.72	0.89	0.69	0.88
Sb	0.63	0.99	0.81	0.85	0.85	0.98	0.98	0.99	0.94	0.05	0.99	0.50	0.99	0.97	1.00		0.64	0.74	0.52	0.38	0.36	0.95	0.71	0.87	0.68	0.86
Pb	0.59	0.73	0.76	0.84	0.89	0.75	0.70	0.71	0.85	0.21	0.69	0.75	0.68	0.80	0.70	0.70		0.62	0.27	0.81	0.73	0.77	0.91	0.64	0.78	0.70
V	0.28	0.39	0.31	0.49	0.35	0.38	0.38	0.41	0.37	0.22	0.40	0.20	0.42	0.40	0.39	0.38	0.44		0.45	0.54	0.52	0.73	0.71	0.72	0.65	0.75
Cr	0.20	0.41	0.28	0.30	0.27	0.38	0.39	0.38	0.44	0.84	0.39	0.60	0.38	0.49	0.39	0.38	0.40	0.11		0.31	0.32	0.49	0.37	0.53	0.44	0.54
Rb	0.64	0.81	0.74	0.92	0.92	0.83	0.79	0.78	0.89	0.07	0.75	0.64	0.75	0.82	0.76	0.77	0.90	0.40	0.27		0.96	0.56	0.82	0.57	0.83	0.65
Cs	0.50	0.65	0.56	0.80	0.82	0.67	0.64	0.61	0.77	0.11	0.58	0.65	0.58	0.70	0.60	0.61	0.84	0.44	0.23	0.95		0.51	0.74	0.53	0.77	0.61
Ga	0.60	0.99	0.81	0.85	0.85	0.99	0.99	0.98	0.95	0.06	0.98	0.53	0.98	0.97	0.99	0.98	0.71	0.38	0.40	0.79	0.63		0.82	0.90	0.82	0.91
La	0.71	0.87	0.81	0.88	0.94	0.88	0.82	0.85	0.88	0.04	0.83	0.52	0.83	0.84	0.84	0.84	0.87	0.44	0.32	0.89	0.77	0.84		0.79	0.89	0.84
Ce	0.60	0.89	0.80	0.81	0.78	0.90	0.86	0.88	0.81	0.00	0.89	0.30	0.90	0.81	0.89	0.87	0.67	0.36	0.32	0.72	0.54	0.87	0.87		0.83	0.99
Pr	0.68	0.90	0.81	0.89	0.82	0.92	0.89	0.87	0.87	0.01	0.86	0.43	0.86	0.82	0.85	0.85	0.70	0.28	0.31	0.85	0.68	0.87	0.85	0.87		0.88
Nd	0.62	0.91	0.82	0.83	0.82	0.92	0.88	0.91	0.84	0.01	0.91	0.32	0.92	0.84	0.91	0.89	0.70	0.36	0.32	0.76	0.57	0.89	0.90	1.00	0.90	

Table 3

Summaries of principal component analysis for trace metals in coarse, fine and submicron particles observed in Hsuehshan Tunnel. Factor loadings lower than ± 0.4 are not given. Loading factor greater than 0.7 is marked by bold.

	Coarse		Fine			Submicron			
	PC1	PC2	PC1	PC2	PC3	PC1	PC2	PC3	PC4
Al ^a		0.55	0.52		0.68			0.88	
Fe	0.98		0.94			0.82	0.52		
Na		0.81			0.93				
Mg		0.89	0.70		0.66	0.69			
K		0.88	0.77		0.44		0.57		
Ca		0.75	0.81			0.65		0.53	
Ba	0.94		0.95			0.96			
Ti	0.93		0.94			0.73			
Mn	0.97		0.90				0.96		
Ni				0.76				0.56	0.72
Cu	0.98		0.95			0.96			
Zn	0.65	0.42	0.44	0.79			0.97		
Mo	0.99		0.96			0.96			
Cd	0.97		0.92				0.90		
Sb	0.99		0.96			0.90			
Pb	0.58	0.71	0.62	0.61			0.84		
V	0.72								0.92
Rb		0.90	0.73	0.44			0.63		
Ga	0.93		0.96			0.94			
La	0.65	0.68	0.80			0.81			
Ce	0.86		0.86			0.92			
Potential source	Wear debris+ Diesel	Dust+ Gasoline	Wear debris + Dust + Gasoline	Diesel	Dust	Wear debris + Auto catalyst	Diesel	Dust	Fuel oil

Table 4

Ratios of specific elements to Cu of PM in tunnel PM.

Tunnel studies	Size	Fe/Cu	Ba/Cu	Sb/Cu	Sn/Cu	Reference ^b
Hatfield Tunnel (United Kingdom)	PM ₁₀	19	1.23	0.13		1
Marquês de Pombal Tunnel (Portugal)	PM _{0.5-10}	16	0.27	0.08	0.23	2
Tsngstad Tunnel (Sweden)	PM ₁₀	28	0.74	0.18		3
Lundby Tunnel (Sweden)	PM ₁₀	60	1.34	0.24		3
Malraux Tunnel (France)	PM _{2.5}	15		0.14	0.14	4
Squirrel Hill Tunnel (USA) ^a	PM _{2.5}	37	2.48	0.21	0.48	5
Sepulveda Tunnel (USA) ^a	PM _{2.5}	16	2.12	0.88	0.82	6
Loma Largo Tunnel (Mexico)	PM _{2.5}	7	0.13	0.76	0.49	7
Jãnio Tunnel (Brazil)	PM _{2.5}	20		0.12		8
Belway Rodonael Mário Covas Tunnel (Brazil)	PM _{2.5}	45		0.36		8
Shing Mun Tunnel (Hong Kong)	PM _{2.5}	17	0.58	0.14	0.29	9
Zhuijiang Tunnel (China)	PM _{2.5}	28	1.08			10
Hsuehshan Tunnel (Taiwan)	PM _{1.8-10}	14	0.80	0.14	0.09	This study
	PM _{1-1.8}	14	1.07	0.16	0.09	
	PM ₁	15	1.10	0.16	0.11	

^a. The ratios of Squirrel Hill Tunnel and Sepulveda Tunnel are obtained from the ratios of elemental emission factors.

^b. 1.Lawrence et al. (2013); 2.Pio et al. (2013); 3.Sternbeck et al. (2002); 4. Fabretti et al. (2009); 5.Grieshop et al. (2006); 6.Gillies et al. (2001); 7.Mancilla and Mendoza (2012); 8Brito et al. (2013); 9.Cheng et al. (2010); 10.He et al. (2008).

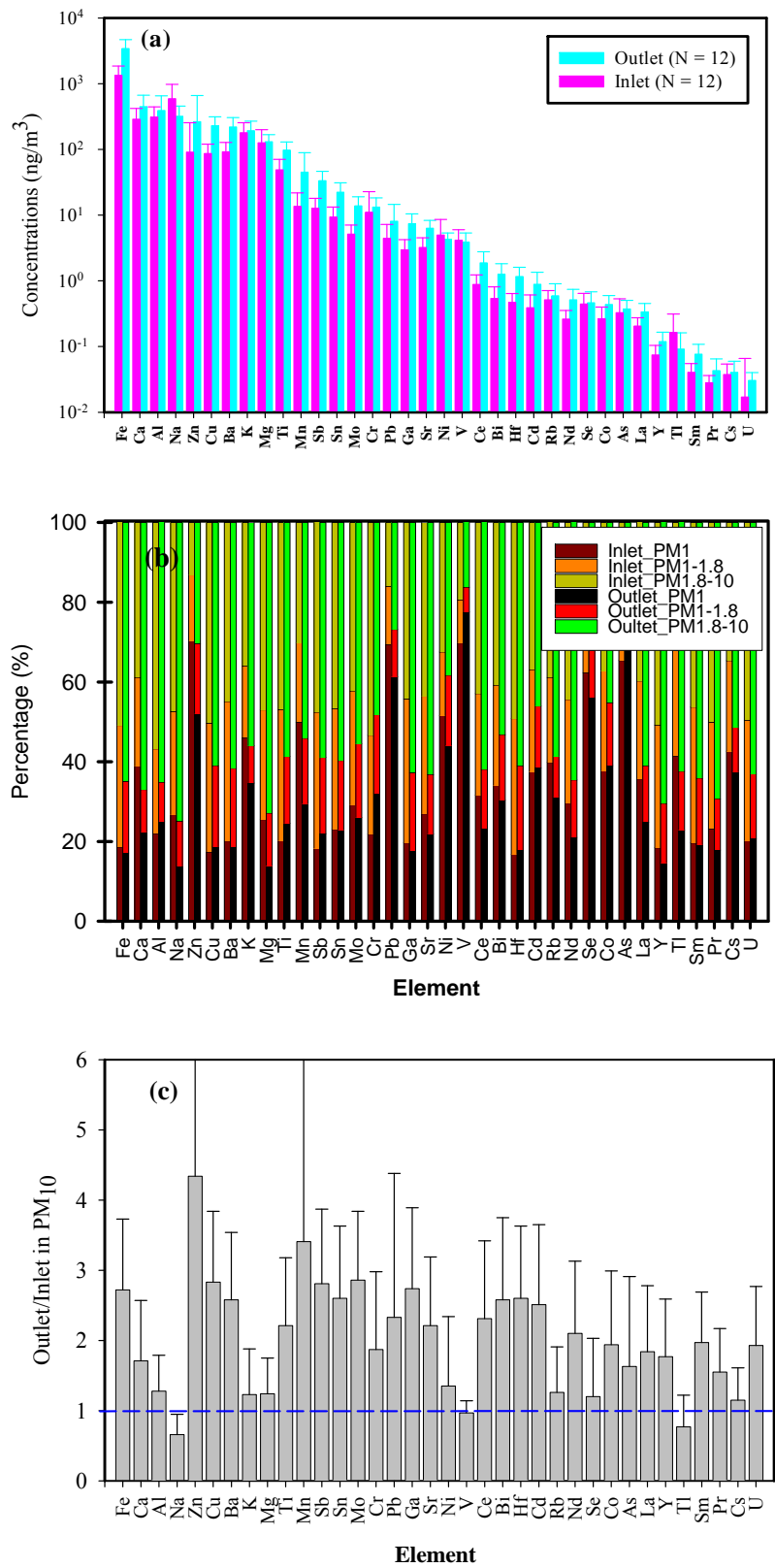


Figure 1.

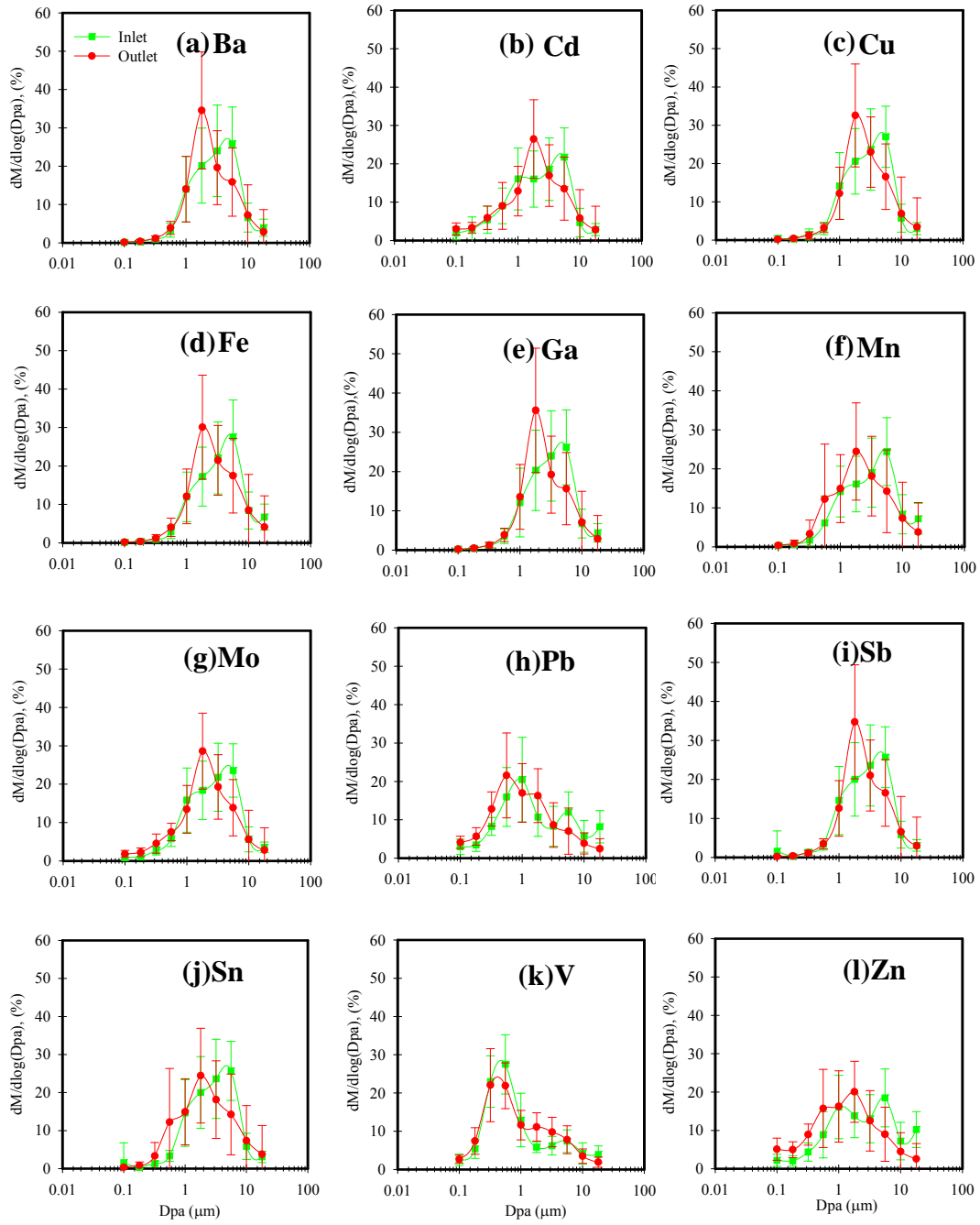


Figure 2.

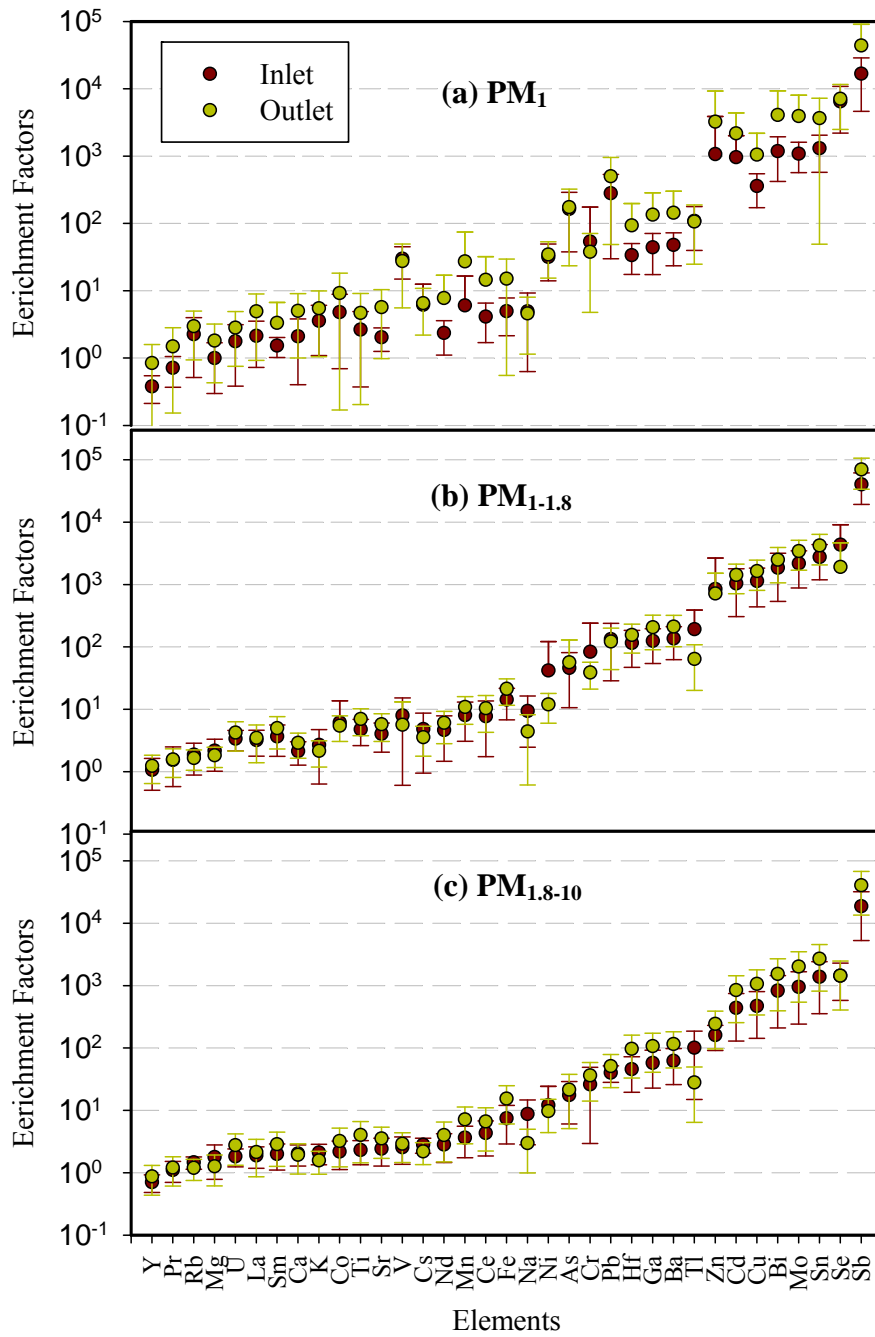


Figure 3.

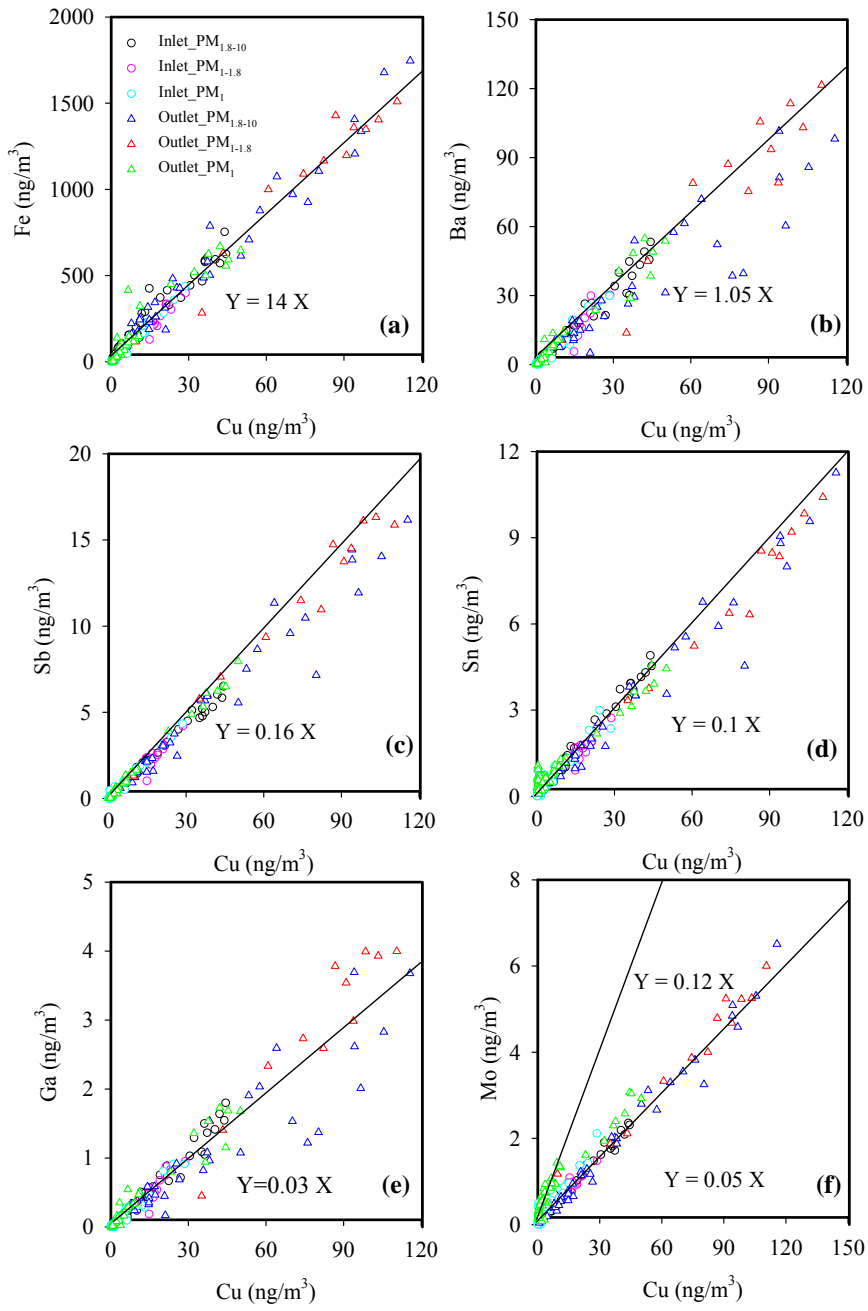


Figure 4.

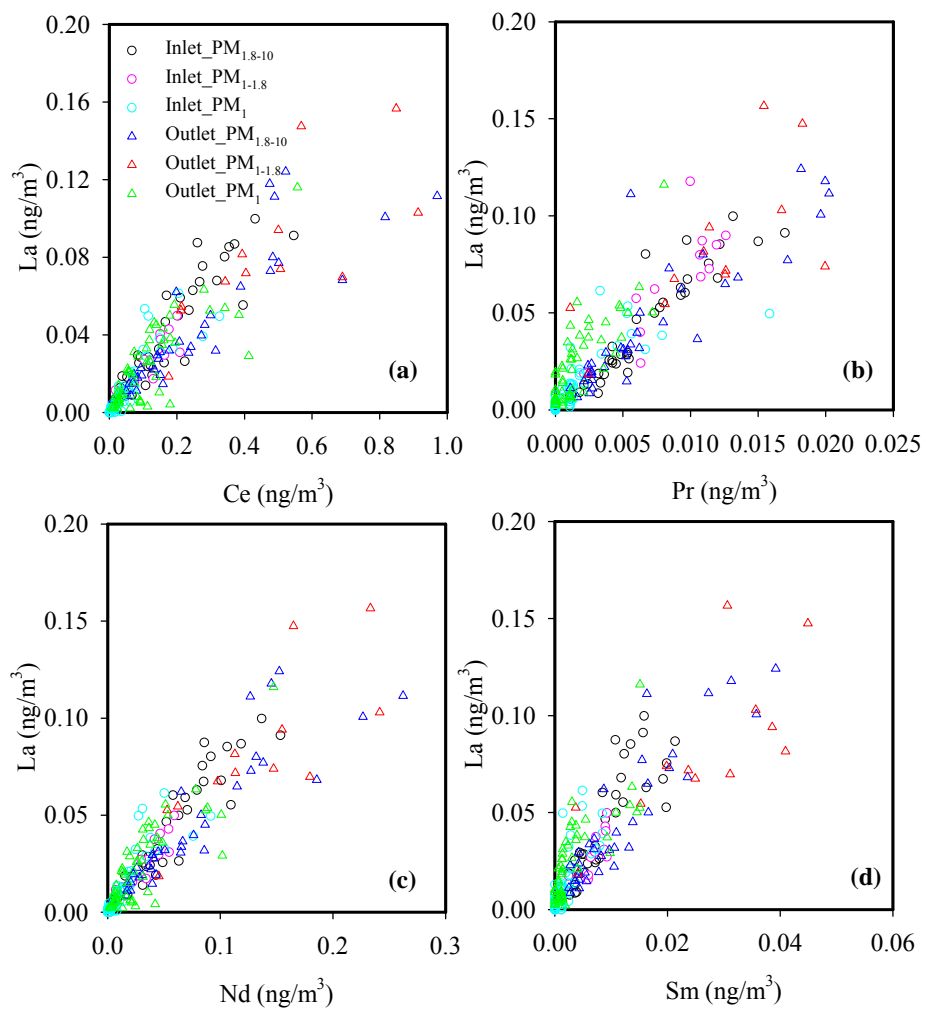


Figure 5.